Original Article

Simulation of the 6 MV Elekta Synergy Platform linac photon beam using Geant4 Application for Tomographic Emission

Samir Didi[1,2], Abdelilah Moussa[1,3], Tayalati Yahya[1], Zerfaoui Mustafa[1,2]

[1]Department of Physics, Laboratory of Physics of Radiation and Matter, Faculty of Sciences, University Mohammed First, [2]Department of Physics, Regional Hassan II Oncology Center, Oujda 60000, [3]Department of Physics, National School of Applied sciences of Al-Hoceima, Morocco

Received on: 12-01-2015 **Review completed on:** 10-06-2015 **Accepted on:** 28-06-2015

ABSTRACT

The present work validates the Geant4 Application for Tomographic Emission Monte Carlo software for the simulation of a 6 MV photon beam given by Elekta Synergy Platform medical linear accelerator treatment head. The simulation includes the major components of the linear accelerator (LINAC) with multi-leaf collimator and a homogeneous water phantom. Calculations were performed for the photon beam with several treatment field sizes ranging from 5 cm × 5 cm to 30 cm × 30 cm at 100 cm distance from the source. The simulation was successfully validated by comparison with experimental distributions. Good agreement between simulations and measurements was observed, with dose differences of about 0.02% and 2.5% for depth doses and lateral dose profiles, respectively. This agreement was also emphasized by the Kolmogorov–Smirnov goodness-of-fit test and by the gamma-index comparisons where more than 99% of the points for all simulations fulfill the quality assurance criteria of 2 mm/2%.

Key words: Geant4 Application for Tomographic Emission/Geant4, grid, Monte Carlo, radiotherapy

Introduction

Since a couple of decades, Monte Carlo simulations for radiation transport have been extensively used in dosimetry and medical radiation physics as an alternative to the analytical calculations. Very accurate results are obtained with these techniques thanks to the powerful distributed grid computing resources.[1-9]

In this paper, we present the simulation of the Elekta Synergy Platform medical linear accelerator treatment head using the release v6.2 of GATE (Geant4 Application for Tomographic Emission) Monte Carlo simulation platform.[10-19] The goal is to calculate the dose distributions in a water phantom keeping the accuracy of results within 2%.

GATE is advanced C++ open-source software developed by the international OpenGATE collaboration for nuclear medicine simulation.[10] The initial focus (in 2004) was devoted to positron emission tomography and single photon emission tomography, but later on has been extended to cover the radiotherapy field. Built on the top of Geant4[20-26] simulation toolkit, GATE inherits all the well-validated physics models and provides the users with a versatile integrated specific components to easily handle a complex geometry and sources, to extract and to treat the relevant information from the simulation.

Address for correspondence:
Prof. Tayalati Yahya,
LPMR, University Mohammed First,
P. O. Box 717, Oujda 60000, Morocco.
E-mail: tayalati@©cern.ch

Access this article online	
Quick Response Code:	Website: www.jmp.org.in
	DOI: 10.4103/0971-6203.165077

How to cite this article: Didi S, Moussa A, Yahya T, Mustafa Z. Simulation of the 6 MV Elekta Synergy Platform linac photon beam using Geant4 Application for Tomographic Emission. J Med Phys 2015;40:136-43.

All these features participated in the growing and fast evolving of GATE use for the wide medical physics applications. GATE in its recent versions plays now a key role in the design of new medical imaging devices in the optimization of acquisition protocols and in dose calculations for radiotherapy.

The rest of the paper is organized as follows: In section 2, we will focus on the modeling of the geometry of the Elekta Synergy Platform accelerator, where our simulation strategy is fully described. The next section covers the results and the comparison of simulated and measured dose profiles distributions. Finally, in section 4, conclusions are drawn.

Materials and Methods

Reference data

All measurements were taken at our Regional Oncology Center, on Synergy Platform Elekta, Radiotherapy Unit. The lower energy photon beam (X-6 MV) was used with a reference dose rate of 400 MU/min. Data were obtained at a source-surface distance (SSD) of 100 cm using a cylindrical thimble ionization chamber, type 9732-2 having an active volume of 0.125 cm^3, mounted over a motorized guide in an resistance temperature detectors 3D water phantom model 9750 made in Multidata Systems Germany (Model 9750).

Accelerator geometry

Based on the vendor detailed information, we simulated the head of the linear accelerator, by the use of GATE. Figure 1 illustrates the global head structure of the linear accelerator and the water phantom considered in this study. Simulated components include:

X-ray target - creates bremsstrahlung X-rays with a thin tungsten and rhenium disk approximately 0.9 mm tick. Remaining primary electrons are absorbed in a graphite absorber inside the target.

Primary conical collimator - made of tungsten alloy, about 10.1 cm high, located just below the X-ray target used to collimate the X-ray in the direction of the treatment field and to reduce the leakage radiations from the X-ray sources.

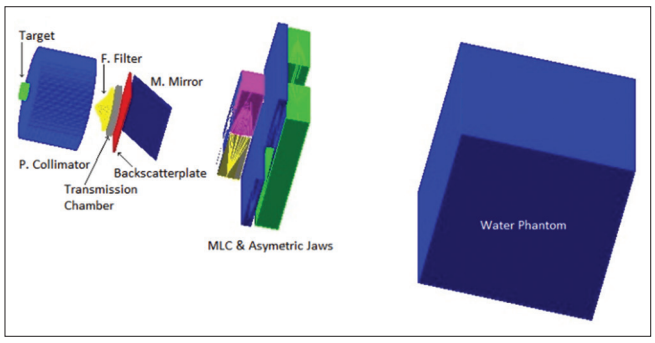

Figure 1: The schematic representation of Elekta medical linear accelerator and water phantom simulated in our study. The components are not to scale

X-ray beam flattening filter - made of stainless steel, having an accurately defined surface configuration, attached to the lower end of the primary collimator and providing uniform radiation intensity distribution across X-ray fields.

Transmission chambers - used for beam control and for the monitoring of photon and electron radiation beam output. A ceramic motherboard and a number of signal and polarizing Mylar films separated by spacers made of aluminum alloy or ceramic.

Backscatter plate - used to avoid the excessive backscattered radiations from the secondary collimators.

Thin Mylar mirror - placed on the beam central axis under the dose monitor to enable patient set-up and show the position of the radiation beam.

Multi-leaf collimator - used for precise delivery of treatment and for most accurate conformal beam shaping for treatments.

Asymmetric jaws - made of tungsten and used to set the overall size of the treatment field.

Water phantom - 50 cm × 50 cm × 50 cm cube is defined at 100 cm from the target with 1 cm plastic outer covering layer except in beam entrance plane.

Table 1: Complete structural configuration of linac modeling along with the corresponding GATE components

Linac component	*GATE components*
X-ray target	/gate/linac/daughters/insert (Cylinder)
Primary conical collimator	/gate/linac/daughters/insert (Cone)
X-ray beam	/gate/linac/daughters/insert (Cylinder)
Flattening filter	/gate/flattening_filter/daughters/insert (Cone)
Transmission chambers	/gate/linac/daughters/insert (Cylinder)
Backscatter plate	/gate/linac/daughters/insert (Box)
Thin Mylar mirror	/gate/linac/daughters/insert (Box)
Phase space	/gate/linac/daughters/insert (Cylinder)
Multi-leaf Collimator	/gate/linac_MLC/daughters/insert (Box) /gate/linac_MLC_Leaf1_Left/daughters/insert (general_trpd and cylinder)
Asymmetric jaws	/gate/linac_Gantry/daughters/insert (Box) /gate/backupX_1/daughters/insert (general_trpd and cylinder)
Water phantom	/gate/world/daughters/insert (Box)

GATE: Geant4 Application for Tomographic Emission

Table 1 shows the complete structural configuration of linac modeling along with the corresponding components used in GATE.

Simulation strategy

The GATE simulations were performed in two steps as illustrated in Figure 2. First, the patient-independent part of the accelerator that corresponds to the accelerator head above the secondary collimator was simulated. Second, a phase space was built. In actual, GATE offers the possibility to attach a phase space to any geometry in the simulation. Here, such phase space was considered as a cylinder of 20 cm diameter and 1 mm tick used to store all the cinematic and production properties of particles above the secondary collimator. Once achieved, inputs from the phase space were used to initiate the simulation of the patient-dependent part.

Phase space build-up is highly CPU time-consuming. To perform this step in a reasonable time scale, the corresponding task has been split into sub-tasks and run on the grid computing resources located at the IN2P3 computing center facility with 20,000 Cores equivalent to 208 866 HEPSpec06.[27] A subset of phase space output files were compressed and transferred to our national grid site[28] where the next step of the simulation is performed using our grid computing resources. The final step consists in exploring the events using ROOT[29] data analysis platform.

GATE has been set up using the default parameters with an additional StepLimiter of 1 mm in water corresponding to the energy cuts of roughly 350 keV and 5 keV for both electrons and positrons, and for photons, respectively.

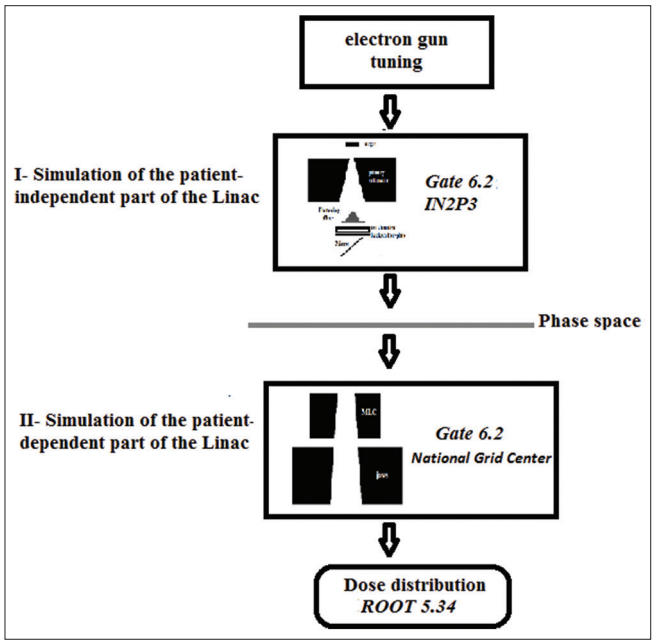

Figure 2: The steps taken to simulate the linac. The gray line represent the electron phase space outputs, and all the simulation programs and CPU location used are given in italics

As most of the particles that reach the phantom are bremsstrahlung gammas, the selective bremsstrahlung splitting,[30] nonbiased variance reduction technique was used to accelerate the simulation process.

In our simulation, the bremsstrahlung splitting was performed with two criteria:

- Energy threshold on primaries: Should be >6.6 MeV to enable the split
- Angle threshold on secondary: No photon with angle >60° was generated.

Basically, secondary gammas particles generated by bremsstrahlung are splitted N times, so that each time a bremsstrahlung gamma is created, other N-1 gammas are generated at the same position, with weight 1/N, re-sampling the energy, and angle distribution. Variance technique has been used here with a splitting factor of 100 as described in Grevillot *et al.*[6]

Furthermore, GATE KillActor was employed to reduce the CPU time of the accelerator simulation. The particles tracking are confined to regions where they are actually influential on the dosimetric parameters in the water phantom.

It has been shown that the choice of the mean energy of primary electron beam hitting the target affects considerably depth dose and dose profile curves. Furthermore, in contrast to depth dose curves, dose profile curves are also influenced by the radial intensity of initial electron beam for a large field size.[31,32]

To achieve reliable results in which Monte Carlo's predicted outputs match measured data, the critical parameters of the primary electron beam, including its mean energy and spatial distribution must be tuned very accurately. These parameters were adjusted very carefully according to the reference method described in Verhaegen and Seuntjens.[1]

Standard 10 cm × 10 cm field size was used to adjust the electron source parameters. We considered a Gaussian distribution for both the energy spectrum and the spot size. The best mean energy parameter was found using several simulations performed to scan the mean energy interval (5.5 MeV, 7.5 MeV) around the firm reference value.

Similar approach was applied to the full width at half maximum (FWHM) electron spot interval of 0 mm, 5 mm to optimize the beam spot size.

In what follows, results are presented for several treatment field sizes ranging from 5 cm × 5 cm to 30 cm × 30 cm. Comparison to real data is made using both depth dose profiles (PDDs) and in-plane profiles at 5 cm, 10 cm, 20 cm, and 30 cm depths.

The GATE simulation performed on the grid lasted approximately 17 h. We simulated a total of three billion (3×10^9) primary electrons used in the work presented here.

Dose distributions are calculated in water phantom, positioned at 100 cm SSD with dosel (dose scoring voxel) of 5 mm × 5 mm × 5 mm to mimic the thimble ionization chamber active volume.

In order to build a robust analysis of calculations against measurements, the simulations were assessed by the means of three tests. Each of them has its own advantages and limitations; they were considered together to complete each other.

First, our results were evaluated by calculating the standard mean point-to-point dose error, with equation:

$$\varepsilon = \frac{1}{N}\sum_i \frac{|d_i - dref_i|}{dref_i}, \quad (1)$$

Where ε is the mean point-to-point error, i corresponds to a curve point index, N is the number of points, d_i is the dose computed at point i and $dref_i$ is the reference dose measured at point i.

The use of the point-to-point errors in low dose areas could lead to high overall errors, therefore, in the case of lateral profiles, agreement with measurements was also estimated by:

$$\varepsilon_N = \frac{1}{N}\sum_i \frac{|d_i - dref_i|}{dref_{\max}}, \quad (2)$$

which normalizes errors to the maximum measured dose $dref_{max}$ and counterweights the point to point errors according to the dose deposited.

This test is the most intuitive one and straightforward. However, a small ionization chamber alignment error could induce large dose differences, especially in the high dose gradient region.[33-35]

More information was derived from a second comparison with the nonparametric Kolmogorov–Smirnov (K–S) test.[36] We calculated the distance $d = |d_m - d_S|$ between the experimental and simulated distributions and the probability of compatibility between the two compared distributions:

$$P_{KS}(d) = Q_{KS}(\sqrt{N}d) \quad (3)$$

Where $Q_{KS}(x) = 2\sum_{j=1}^{+\infty}(-1)^{j-1}e^{-j^2}x^2$.

The K–S test has an interesting advantage in which it does not require any assumptions about the data. Despite of its simplicity and advantages, the K–S test also has several important limitations. The most serious one is its tendency to be more sensitive near the center of the distribution than at the tails.

We found it interesting to perform a third test by calculating the gamma-index. Recently, this test became the gold standard for the comparison between measured and calculated dose distributions.[37-39] Even though its interpretation is clinically less intuitive, the gamma index calculation complements the previous tests by its ability to produce a quantitative measure based on both dose and spatial criteria.

The gamma-index is defined for each measurement point r_m as:

$$\gamma(r_m) = \min\{\Gamma(r_m, r_c)\} \ \forall\{r_c\}, \quad (4)$$

where $\Gamma(r_m, r_c) = \sqrt{\frac{(r_m - r_c)^2}{\delta r_m^{\,2}} + \frac{(d_m - d_c)^2}{\delta d_m^{\,2}}}$ and r_c represents the spatial location of the calculated distribution relative to the measured one.

The main limitation of this last tool comes from its sensitivity to the dose grid resolution. Here, the number of points passing the very accurate quality assurance criteria of $(\delta r_m = 2mm / \delta d_m = 2\%)$ is considered, 100% of the points pass the 2%/2 mm comparison if $\gamma(r_m) > 1 \ \forall\{r_m\}$.

Due to the lack of primary event interactions in the tail of the penumbra, the uncertainty was larger, and these points were not considered. Therefore, to avoid a nonrepresentative increase of the statistical uncertainties, all points in this low dose area having a dose lower than 10% of the maximum dose was not considered.

Results and Discussion

A mean electron beam energy of 6.7 MeV and a FWHM electron spot of 3 mm were found to be in a good agreement with the measurements. As recommended in literature, the FWHM energy was set to 3%.[32]

The mean electron energy of 6.7 MeV found for this specific Elekta model is higher than those found in

Table 2: Mean energy and FWHM of the incident electron beam distribution from the simulation of different Elekta models[40-43]

Elekta linac accelerator type	*E (MeV)*	*FWHM (mm)*
Synergy	6.1	5
SL-25	6.4	
Precise	6.3	1.1
Precise	5.8	3

FWHM: Full width at half maximum

literature [Table 2]. However, this mean value is close to that of 6.5 MeV provided by the manufacturer together with their detailed specifications of the accelerator's head components.

To validate the properly tuning of the beam, the quality index tissue phantom ratio in water at depths of 20 and 10 cm ($TPR_{20,10}$) for the 10 cm square field is reported and compared between experimental measurements and simulation as shown in Table 3. This parameter is relevant to express the quality of high photon beam according to international recommendations (IAEA TRS398).

Simulated TPR was obtained from the simple relation:[44]

$$TPR_{20/10} = 1.2661 \times PDD_{20/10} - 0.0595$$

Where $PDD_{20/10}$ is the ratio ionization for 10 cm × 10 cm field at depths of 20 cm and 10 cm, obtained from the simulated profile depth dose for the field size 10 cm × 10 cm.

Deviation between measurement and GATE data for $TPR_{20,10}$ value is smaller than 1.2%. This shows that the primary source energy was tidily tuned.

The beam quality is also specified in terms of the output factors. They are known to depend in a fairly unpredictable way on the electron energy and the geometry of the jaws, applicator, and the final field defining cutout. The output factors are the ratio of the dose rate of a given field size to the dose rate of the reference field size, both at the depth of 10 cm (IAEA TRS398). Table 4 shows the comparison of simulated and measured output factors for square field sizes ranging from 5 cm × 5 cm to 30 cm × 30 cm. Output factors show a good agreement between simulation and measurements with a maximum discrepancy of 0.85%.

Table 3: Comparison of measured and simulated $TPR_{20,10}$ value

Filed (cm²)	*$TPR_{20,10}$ Measured*	*$TPR_{20,10}$ GATE*
10×10	0.684	0.677

GATE: Geant4 Application for Tomographic Emission, $TPR_{20,10}$: Tissue phantom ratio in water at depths of 20 and 10 cm

Table 4: Comparison of simulated and measured output factors for square field sizes ranging from 5 cm × 5 cm to 30 cm × 30 cm

Filed (cm²)	*Measured output factors*	*Simulated output factors*	*Error %*
5×5	0.94681	0.95487	0.85
10×10	1	1	0
20×20	1.03878	1.04106	0.21
30×30	1.05854	1.05582	0.25

Let us now examine the quality of the results we got for depth and lateral dose profiles.

In Figure 3, simulated PDDs are compared to the experimental ones. Profiles were obtained with 6 MV photon beam at 100 cm of SSD in water phantom using square field sizes ranging from 5 cm × 5 cm to 30 cm × 30 cm. Each distribution is normalized to their maximum value.

It can be concluded from the figure that the Monte Carlo model for 6 MV photon beam accurately matches the measured data.

We summarize the agreement between calculations and measurements according to the statistical tests considered in this study as shown in Table 5. Both the experimental data and the GATE simulation results were divided into two regions of interest, the build-up region in which the dose reaches its maximum value at a depth Z_{max} and the tail region beyond the Z_{max}. The agreement between the two distributions within each of these two regions is reported. As for the calculation of the K–S probability and the gamma index, all depths for PDDs including build-up region were considered.

PDDs from Monte Carlo simulations match the measured data within 0.02%, and it can be verified in any region considered that the K–S test points out a good agreement between experimental data and GATE simulations with a global $P = 1$ in any case. Furthermore, the percentage of points passing the gamma-index criteria of 2 mm/2% when comparing calculated and measured depth dose distributions are of 99% and therefore strengthens this agreement result.

The lateral dose profiles at 5, 10, 20, and 30 cm depths, for the 6 MV beam and SSD at 100 cm, in water phantom in the case of a square field sizes ranging from 5 cm × 5 cm to 30 cm × 30 cm are shown in Figure 4. Lateral profiles obtained with experimental measurements were normalized to the dose value on the beam axis while the ones obtained with GATE were normalized to the mean value in the flat zone.

The results of the statistical comparison of the simulated lateral profiles with the measured ones are gathered in Table 6.

Overall, one can see that lateral doses profiles are in good agreement with measurements. The largest statistical uncertainties occurred for the 5 cm × 5 cm radiation field at 5 cm depth with up to 5.93% of discrepancy for ε. As discussed above, for small fields, only few points are evaluated, errors in the high dose-gradient regions increase significantly the overall error. In such situation, one must refer instead to ε_N is more appropriate to evaluate the

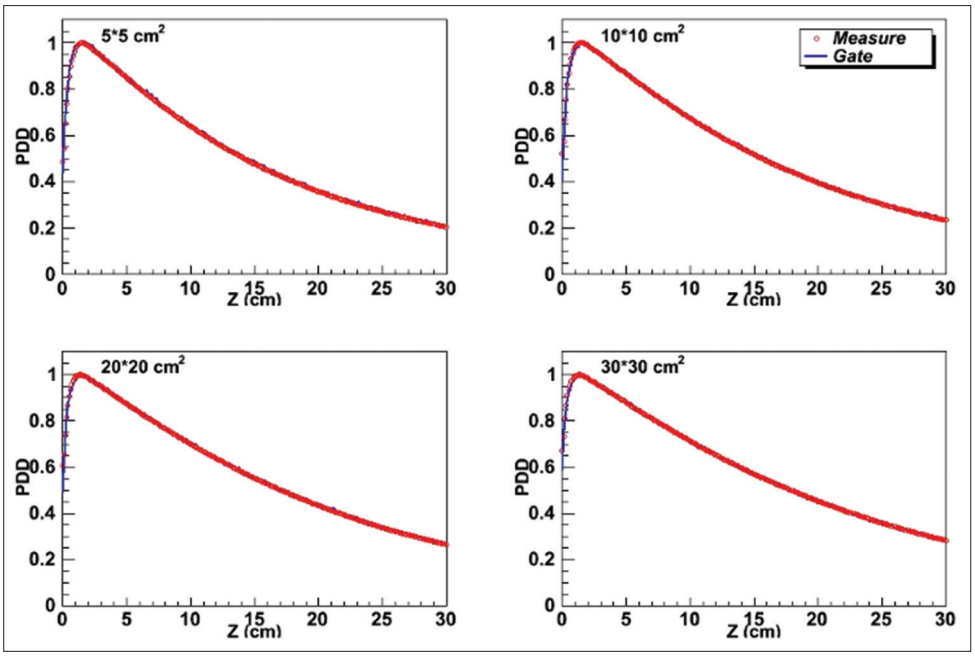

Figure 3: Comparison of calculated and measured depth dose for 6 MV photon beam for field sizes ranging from 5 cm × 5 cm to 30 cm × 30 cm. Red circles refer to measured data and the blue solid lines refer to Gate Monte Carlo results

Table 5: Comparison of the simulated PDDs with the measured ones for the square field sizes ranging from 5 cm × 5 cm to 30 cm × 30 cm

Filed (cm²)	*Depth (cm)*	ε	d_{ks}	P_{ks}	γ
5×5	$Z \leq Z_{max}$	0.0127	0.0045	1	99
	$Z > Z_{max}$	0.0147	0.0027		
10×10	$Z \leq Z_{max}$	0.0078	0.0055	1	99
	$Z > Z_{max}$	0.0071	0.0014		
20×20	$Z \leq Z_{max}$	0.0110	0.0053	1	99
	$Z > Z_{max}$	0.0045	0.0008		
30×30	$Z \leq Z_{max}$	0.0168	0.0047	1	99
	$Z > Z_{max}$	0.0001	0.0004		

PPD: Percentage depth dose

simulation. In this case, the largest statistical uncertainties occurred for the profiles reaches only 2.5%.

For all fields, the K–S test emphasizes a good agreement between experimental lateral dose profiles and GATE simulated ones with a maximum probability in any case. This result is enhanced once again by the gamma-index comparison, which shows excellent agreement for the simulations. All curves passed the comparison with a maximum score of 100%.

The purpose of this study is fulfilled. The GATE simulation excellently matches the measured data. All the comparisons state the absence of statistical difference between the experimental and Monte Carlo profiles. One can see that simulated PDDs agree with the measurements within 0.01%. The simulation fits also accurately the measured lateral dose profiles with no more than 1.8% of error uncertainties, except for the small filed at 5 cm and 30 cm depths, where 2.45% and 2.4% of errors were registered, respectively. But this is typically accepted as a satisfactory result for the Monte Carlo dosimetric control.

Good agreement is also obtained with the K–S comparison of the experimental distributions with the simulated ones. The percentage of points passing the gamma-index criteria of 2 mm/2% when comparing calculated and measured dose distributions is generally >99% for the studied cases.

This complex simulation that would take more than a year on a normal processing unit was performed here in <1 day. It is also interesting to note that the selective bremsstrahlung splitting used in our study has sped up about 6 times the accelerator head simulation without biasing the results. All this, confirms the goodness of our simulation and shows the efficiency of the strategy adopted in reducing CPU time without changing the reality of the problem.

Conclusion

This paper presents GATE simulation model developed to perform an accurate simulation of dose profiles from a 6 MV Elketa Synergy Platform medical linac.

Given the flexibility of GATE, the key components of the accelerator head have been easily modeled based on the manufacturer's specifications. The results obtained with the

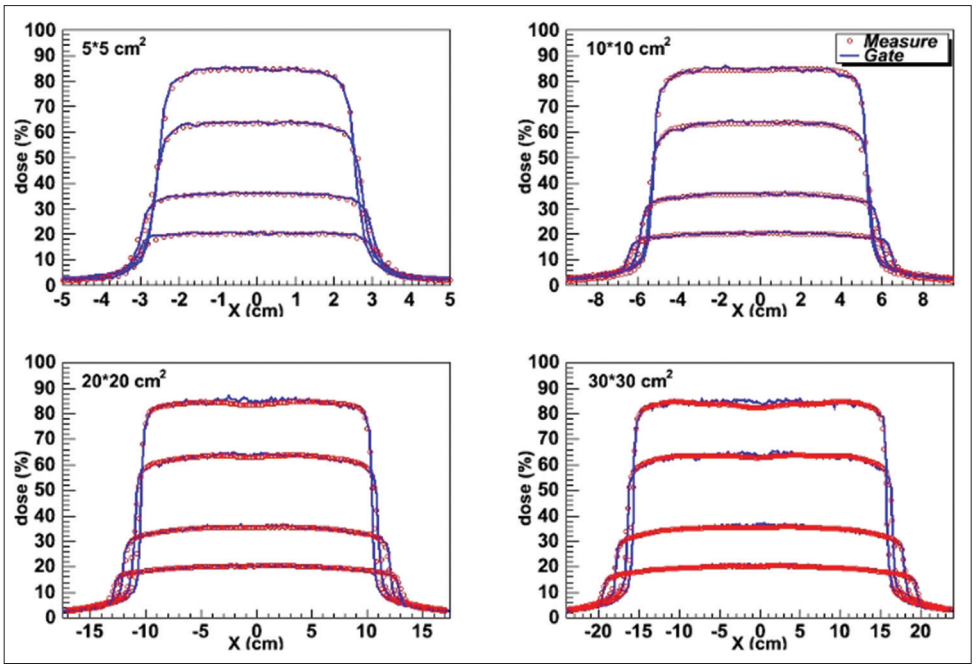

Figure 4: Lateral dose profiles at 50, 100, 200 mm, and 300 mm depths for the square field sizes ranging from 5 cm × 5 cm to 30 cm × 30 cm, with a 6-MV beam. Red circles refer to measured data, and the blue solid lines refer to Monte Carlo results

Table 6: Comparison of the simulated lateral dose profiles with the measured ones for the square field sizes ranging from 5 cm × 5 cm to 30 cm × 30 cm

Filed (cm²)	*Depth (cm)*	ε	ε_N	d_{ks}	P_{ks}	γ
5×5	5	5.9311	2.4527	0.0052	1	100
	10	4.1897	1.7656	0.0052		
	20	2.8840	1.8766	0.0098		
	30	3.0232	2.3807	0.0052		
10×10	5	3.7733	1.8736	0.0076	1	100
	10	2.2159	1.0924	0.0044		
	20	2.7745	1.8079	0.0059		
	30	1.8882	1.5257	0.0029		
20×20	5	3.1983	1.6003	0.0066	1	100
	10	2.2032	1.3003	0.0030		
	20	1.5305	1.1552	0.0031		
	30	1.6234	1.3449	0.0059		
30×30	5	2.3799	1.5183	0.0061	1	100
	10	2.1054	1.3826	0.0055		
	20	1.7887	1.3812	0.0045		
	30	1.3072	1.2032	0.0040		

simulation in terms of depth dose and lateral beam profiles for different therapeutic field sizes in a water phantom show an excellent agreement with the measured data found with an incident mean electron energies of 6.7 MeV and a FWHM electron spot of 3 mm.

This preliminary study demonstrates that GATE can be used for radiation therapy applications. It's simple macro file structure significantly facilitates the elaboration of Geant4 simulations. Furthermore, the presented results allow the applicability of the obtained phase space to more complex and clinically relevant situations.

Further validation will be performed with different energies, complex MLC fields and with dynamic IMRT irradiation fields.

Acknowledgments

This project is funded by the National Center for Scientific and Technical Research CNRST (URAC07), the High Energy Physics Cluster (RUPHE) and the Spanich-Moroccans PCI2012 (A1/035250/11). The authors would like to thank the openGATE collaboration for providing the toolkit and examples, regular updates, documentation, and the online user forum. The authors would also like to thank Prof. Gorge Dietmar for useful discussions, Elekta's research director Kevin Brown for the given information and Dr. Mohamed Dihi for the English corrections.

Financial support and sponsorship

This project is funded by the National Center for Scientific and Technical Research CNRST (URAC07), the High Energy Physics Cluster (RUPHE) and the Spanich-Moroccans PCI2012 (A1/035250/11).

Conflicts of interest

There are no conflicts of interest.

References

1. Verhaegen F, Seuntjens J. Monte Carlo modelling of external radiotherapy photon beams. Phys Med Biol 2003;48:R107-64.

2. Reynaert N, Van der Marck S, Schaart D, Van der Zee W, Tomsej W, Van Vliet- Vroegindeweij C, *et al*. Monte Carlo Treatment Planning: An introduction. Report 16 of the Netherlands Commission on Radiation Dosimetry 2006.
3. Sardari D, Maleki R, Samavat H, Esmaeeli A. Measurement of depth-dose of linear accelerator and simulation by use of Geant4 computer code. Rep Pract Oncol Radiother 2010;15:64-8.
4. Seco J, Verhaegen F. Monte Carlo Techniques in Radiation Therapy, W Hendee, Series Editor, CRC Press, Taylor and Francis Group, Boca Raton, FL, 2013; ISBN 9781466507920.
5. Ahnesjö A, Aspradakis MM. Dose calculations for external photon beams in radiotherapy. Phys Med Biol 1999;44:R99-155.
6. Grevillot L, Frisson T, Maneval D, Zahra N, Badel JN, Sarrut D. Simulation of a 6 MV Elekta Precise Linac photon beam using GATE/GEANT4. Phys Med Biol 2011;56:903-18.
7. Cornelius I, Hill B, Middlebrook N, Poole C, Oborn B, Langton C. Commissioning of a Geant4 based treatment plan simulation tool: Linac model and dicom-rt interface. 29th European Society for Therapeutic Radiology and Oncology Conference, September 2010, Barcelona. Arxiv preprint arXiv:1104.5082.
8. Aubin JS, Steciw S, Kirkby C, Fallone BG. An integrated 6 MV linear accelerator model from electron gun to dosein a water tank. Med Phys 2010;37:2279-88.
9. Benhalouche S, Visvikis D, Le Maitre A, Pradier O, Boussion N. Evaluation of clinical IMRT treatment planning using the GATE Monte Carlo simulation platform for absolute and relative dose calculations. Med Phys 2013;40:021711.
10. Jan S, Benoit D, Becheva E, Carlier T, Cassol F, Descourt P, *et al*. GATE V6: A major enhancement of the GATE simulation platform enabling modelling of CT and radiotherapy. Phys Med Biol 2011;56:881-901.
11. Jan S, Santin G, Strul D, Staelens S, Assié K, Autret D, *et al*. GATE: A simulation toolkit for PET and SPECT. Phys Med Biol 2004;49:4543-61.
12. Strul D, Santin G, Lazaro D, Breton V, Morel C. GATE (Geant4 Application for Tomographic Emission): A PET/SPECT general-purpose simulation platform". Nucl Phys B (Proc Suppl) 2003;125:75-9.
13. Santin G, Strul D, Lazaro D, Simon L, Krieguer M, Vieira M, *et al*. GATE: A Geant4-based simulation platform for PET, SPECT integrating movement and time management. IEEE Trans Nucl Sci 2003;50:1516-21.
14. OpenGATE Collaboration. Available from: http://www.opengatecollaboration.org. [Last accessed on 2014 Feb 21].
15. Papadimitroulas P, Loudos G, Nikiforidis GC, Kagadis GC. A dose point kernel database using GATE Monte Carlo simulation toolkit for nuclear medicine applications: Comparison with other Monte Carlo codes. Med Phys 2012;39:5238-47.
16. Visvikis D, Bardies M, Chiavassa S, Danford C, Kirov A, Lamare F, *et al*. Use of the GATE Monte Carlo package for dosimetry applications. Nucl Instrum Methods A 2006;569:335-40.
17. Maigne L, Perrot Y, Schaart DR, Donnarieix D, Breton V. Comparison of GATE/GEANT4 with EGSnrc and MCNP for electron dose calculations at energies between 15 keV and 20 MeV. Phys Med Biol 2011;56:811-27.
18. Thiam CO, Breton V, Donnarieix D, Habib B, Maigne L. Validation of a dose deposited by low-energy photons using GATE/GEANT4. Phys Med Biol 2008;53:3039-55.
19. Sadoughi HR, Nasseri S, Momennezhad M, Sadeghi HR, Bahreyni-Toosi MH. A Comparison Between GATE and MCNPX Monte Carlo Codes in Simulation of Medical Linear Accelerator. J Med Signals Sens 2014;4:10-7.
20. Allison J, Amako K, Apostolakis J, Araujo H, Arce Dubois P, Asai M, *et al*. Geant4 developments and applications. IEEE Trans Nucl Sci 2006;53:270-78.
21. Agostinelli S, Allison J, Aamako K, Apostolakis J, Araujo H, Arce P, *et al*. Geant4 – A simulation toolkit. Nucl Instrum Methods A 2003;506:250-303.
22. GEANT4 Collaboration. Available from: http://geant4.cern.ch/. [Last accessed on 2013 Mar 17].
23. Poon E, Seuntjens J, Verhaegen F. Consistency test of the electron transport algorithm in the GEANT4 Monte Carlo code. Phys Med Biol 2005;50:681-94.
24. Foppiano F, Mascialino B, Pia MG, Piergentili M. A Geant4-based simulation of an accelerator's headused for intensity modulated radiation therapy. IEEE 0-7803-8700-7/04; 2004.
25. Poon E, Verhaegen F. Accuracy of the photon and electron physics in GEANT4 for radiotherapy applications. Med Phys 2005;32:1696-711.
26. Constantin M, Perl J, LoSasso T, Salop A, Whittum D, Narula A, *et al*. Modeling the truebeam linac using a CAD to Geant4 geometry implementation: Dose and IAEA-compliant phase space calculations. Med Phys 2011;38:4018-24.
27. IN2P3 Computing Centre Facility. Available from: http://www.cc.in2p3.fr/. [Last accessed on 2014 Apr 23].
28. The National Moroccan Grid. Available from: http://magrid.ma/. [Last accessed on 2014 Apr 23].
29. Brun R, Rademakers F. ROOT – An object oriented data analysis framework", Proceedings AIHENP'96 workshop, Lausanne, September 1996. Nucl Instrum Methods Phys Res A 1997;389:81-6.
30. Kawrakow I, Rogers DW, Walters BR. Large efficiency improvements in BEAMnrc using directional bremsstrahlung splitting. Med Phys 2004;31:2883-98.
31. Chetty IJ, Curran B, Cygler JE, DeMarco JJ, Ezzell G, Faddegon BA, *et al*. Report of the AAPM Task Group No 105: Issues associated with clinical implementation of Monte Carlo-based photon and electron external beam treatment planning. Med Phys 2007;34:4818-53.
32. Fix MK, Keall PJ, Siebers JV. Photon-beam subsource sensitivity to the initial electron-beam parameters. Med Phys 2005;32:1164-75.
33. Low DA, Dempsey JF. Evaluation of the gamma dose distribution comparison method. Med Phys 2003;30:2455-64.
34. Van Dyk J, Barnett RB, Cygler JE, Shragge PC. Commissioning and quality assurance of treatment planning computers. Int J Radiat Oncol Biol Phys 1993;26:261-73.
35. Low DA, Mutic S, Dempsey JF, Gerber RL, Bosch WR, Perez CA, *et al*. Quantitative dosimetric verification of an IMRT planning and delivery system. Radiother Oncol 1998;49:305-16.
36. Eadie WT, Drijard D, James FE, Roos M, Sadoulet B. Statistical Methods in Experimental Physics. North Holland Pub. Co., 1971. p. 269-71.
37. Low DA, Harms WB, Mutic S, Purdy JA. A technique for the quantitative evaluation of dose distributions. Med Phys 1998;25:656-61.
38. Depuydt T, Van Esch A, Huyskens DP. A quantitative evaluation of IMRT dose distributions: Refinement and clinical assessment of the gamma evaluation. Radiother Oncol 2002;62:309-19.
39. Bak J, Choi JH, Kim JS, Park SW. Modified dose difference method for comparing dose distributions. J Appl Clin Med Phys 2012;13:3616.
40. Lye JE, Butler DJ, Ramanathan G, Franich RD. Spectral differences in 6 MV beams with matched PDDs and the effect on chamber response. Phys Med Biol 2012;57:7599-614.
41. Mesbahi A, Mehnati P, Keshtkar A. A comparative Monte Carlo study on 6MV photon beam characteristics of Varian 21EX and Elekta SL 25 linacs. Iran J Radiat Res 2007;5:23-30.
42. Abella V, Miró R, Juste B and Verdú G. Implementation of multileaf collimator in a LINAC MCNP5 simulation coupled with the radiation treatment planing system plunk. Prog Nucl Sci Technol 2011;2:172-5.
43. Grevillot L, Frisson T, Maneval D, Zahra N, Badel JN, Sarrut D. Simulation of a 6 MV Elekta Precise Linac photon beam using GATE/GEANT4. Phys Med Biol 2011 21;56:903-18.
44. Followill DS, Tailor RC, Tello VM, Hanson WF. An empirical relationship for determining photon beam quality in TG-21 from a ratio of percent depth doses. Med Phys 1998;25:1202-5.